Int. J. Electrochem. Sci., 15 **(2020)** 6863 – 6879, doi: 10.20964/2020.07.29

International Journal of
ELECTROCHEMICAL
SCIENCE
www.electrochemsci.org

A Novel Online Parameter Identification Algorithm for Fractional-Order Equivalent Circuit Model of Lithium-Ion Batteries

Lan Li[1], *Huarong Zhu*[2], *Anjian Zhou*[2], *Minghui Hu*[1,*], *Chunyun Fu*[1], *Datong Qin*[1]

[1] State Key Laboratory of Mechanical Transmissions, School of Automotive Engineering, Chongqing University, Chongqing 400044, China.
[2] Chongqing Changan Automobile Co., Ltd., Chongqing 400023, China.
[*]E-mail: minghui_h@163.com

Received: 6 March 2020 / *Accepted:* 21 April 2020 / *Published:* 10 June 2020

Since the parameters of lithium-ion batteries are time-varying, employing a battery model with fixed parameters poses adverse effects to the accuracy of battery state parameter (e.g. state of charge (SOC) and state of health (SOH)) estimation. Thus, it is highly necessary to identify the battery model parameters online to improve the accuracy of battery model. In this study, a fractional-order equivalent circuit model of lithium-ion batteries is established based on second-order RC model and the parameters of the model are identified off-line by the mixed-swarm-based cooperative particle swarm optimization (MCPSO) algorithm. In order to take into account the parameter variations and improve the accuracy of battery model, the model parameters are updated online by the recursive least square (RLS) method to achieve model parameter online identification. Simulation results show that under different cyclic test conditions (i.e. HPPC, DST, and FUDS), the root-mean-square error (RMSE) values of the fractional-order equivalent circuit model based on the real-time update of RLS parameters are less than 9 mV, and the average relative error does not exceed 0.1%, which has higher accuracy and good robustness. The results achieved in this study provide great potential for enhancing estimation accuracies of SOC and SOH for battery management systems (BMSs).

Keywords: lithium-ion battery; fractional-order model; online parameters identification; recursive least squares

1. INTRODUCTION

As the energy source of electric vehicles (EVs), on-board power batteries are of vital importance to the EVs' dynamic performance, economy, and safety, and they are also the critical factor that hinders the evolution of EVs [1-3]. So far, lithium-ion batteries have become the mainstream choice for EV power batteries; this is because these batteries provide the advantages of high energy density, low self-discharge rate, long cycle life, and no memory effect [4-8]. Accurate and effective lithium-ion battery

models are of great significance for improving the estimation accuracy of SOC and SOH, and for facilitating the research on lithium-ion battery performance [9-13].

There exist three main types of lithium-ion battery models: the black box models, the electrochemical models, and the equivalent circuit models (ECMs) [14, 15]. The black box models employ the real vehicle running data to directly perform model training, which makes it conform to the current aging state of the battery. However, the model accuracy depends largely on the quality and quantity of the training data, and the battery operating conditions are complex and varying [16, 17]. As a result, the black-box models are not suitable for hybrid EVs and pure EVs. The electrochemical models better describe battery internal characteristics than other models, however they are composed of numerous equations and parameters, and the simulation accuracy of the battery under complex working conditions is low [18, 19]. The ECMs have been widely used, thanks to their advantages of simple structure, low number of parameters, and easy parameter identification [20-22]. The second-order RC model is a commonly used ECM, and it stands out from the integer-order models as it achieves a good trade-off between prediction accuracy and model complexity [23]. One drawback of the integer-order models is that the electrochemical response inside the battery cannot be well reflected. In view of this shortcoming, Ma et al. [24] used fractional-order impedance elements to further improve the integer-order models. Wang et al. [25] pointed out that the models established by fractional calculus has higher accuracy, compared to the first-order RC model. This is because from the perspective of electrochemical impedance spectroscopy, a circuit composed of fractional-order elements can better fit the impedance characteristics of a battery, and thus has better applications in battery principle analyses, battery modeling, and state estimation [26, 27]. In this paper, a fractional-order ECM is established for lithium-ion batteries, and its schematic is shown in Figure 1.

The accuracy of a fractional-order ECM is dependent on the accuracy of its parameters. Since the battery is a time-varying nonlinear system, most parameters cannot be measured online, and the effectiveness of parameter identification is of special importance. Therefore, parameter identification has also become a key problem that is difficult to solve in the modeling process of lithium-ion batteries. At present, the methods for model parameter identification fall into three categories. The first category is the offline parameter identification methods which are based on offline data, such as linear fitting, least squares (LS) and other methods that cannot achieve identification in real time [28-30]. The parameters identified through offline identification schemes are generally fixed parameters that do not reflect changes in actual operating conditions. Such identification results are only applicable when the battery operating conditions do not change much. In practice, the variations of vehicle speed and battery temperature adversely affect the offline parameter identification results, which in turn leads to large errors in the SOC estimation results. Currently, online identification methods are the dominant methods for battery model parameter identification. These methods are mainly derived from LS, such as RLS [31, 32], deviation compensation recursive least squares [33], and least squares derived algorithms with forgetting factors [34]. However, in the initial stage, the parameter identification results are still inaccurate. The third category of parameter identification methods is indeed a combination of the intelligent optimization algorithms (e.g. particle swarm optimization (PSO) [35] and genetic algorithms (GA) [36]) and the online identification methods. In this category, the intelligent optimization algorithms play a key role in parameter identification, with the online identification methods being complementary.

This type of parameter identification methods can overcome the inaccuracy in the initial stage of online parameter identification. Using the Levenberg-Marquardt method and the experimental data of the Galvanostatic charge-discharge conditions, Santhanagopalan et al. [37] identified the liquid lithium-ion diffusion coefficient, the solid-phase lithium-ion diffusion coefficient of the positive and negative electrodes, and the electrochemical reaction rate constant of the positive and negative electrodes in the quasi-2D mathematical model and the single particle model. The verification shows that when the ambient temperature is at 15 ℃ or 25 ℃, the model parameter identification is effective, and the model output voltage is highly fitted to the measured voltage. However, if the initial parameter is not selected properly, local optimum will appear and result in decrease of model accuracy. Based on the genetic algorithm and the battery model proposed by Doyle et al. [18] and Fuller et al. [38], Forman et al. [36] used lithium-ion battery cycle test data to identify the model parameters, and employed the Fisher information matrix to evaluate the recognizability of the model parameters and the accuracy of the identified model. Finally, the precise of the model was verified by using the actual charging and discharging conditions of the battery. Rahimian et al. [29] used variable forgetting factor recursive least squares method based on the first-order RC ECM for parameter identification of the external input autoregressive model, which solved the problem that with the increase of recursive steps, the accumulated old data gradually increased, making it difficult to modify the new observation data and weakening the effect of parameter updating.

In summary, most existing battery model parameter identification methods are off-line solutions, that is, the identified parameters are invariant. However, in practice, the battery operating current is large and changes rapidly, and the parameter identification accuracy is difficult to be ensured. In addition, the model order and the battery polarization depth are closely related, and the model parameters change with SOC, operating conditions, and internal resistance. As a result, using fixed model parameters can lead to large estimation errors. In order to improve the model accuracy and the system adaptability, it is highly necessary to perform online correction and update of the battery model parameters.

The remainder of the paper is structured as follows. A fractional-order ECM is established for lithium-ion batteries based on the second-order RC model in Section 2. Section 3 describes the off-line identification method of model parameters based on MCPSO algorithm and the on-line identification method based on RLS method. In Section 4, based on the experimental data of FUDS working conditions, MCPSO algorithm is employed to identify the parameters offline, and the initial values of model parameters are obtained. Next, the accuracy of parameter identification is verified under different working conditions, considering that the parameters such as internal resistance of batteries change with time in practical use, the parameters identified are updated online by RLS method to realize online identification of model parameters, and the accuracy of offline identification and online identification of model parameters is compared and analyzed. Finally, conclusions are given in Section 5.

2. MODELING OF LIYHIUM-ION BATTERY

The schematic of the fractional-order ECM is shown in Figure 1, where U_{OCV} indicates the battery open circuit voltage (OCV), U_d is the battery terminal voltage, the current is denoted by I, the

Ohmic internal resistance is represented by R_0 , R_1 and R_2 represent the polarization internal resistances, CPE_1 and CPE_2 are the constant phase elements, and the Wahlberg element is represented by W .

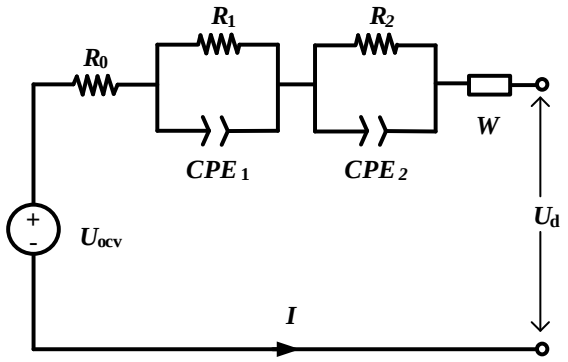

Figure 1. Schematic of fractional-order ECM.

The lithium-ion battery is modeled based on the fractional calculus theory [39], and the lithium-ion battery transfer function of the fractional-order model impedance is presented as follows:

$$\frac{U_d(s)-U_{OCV}(s)}{I(s)}=\frac{R_1}{1+R_1C_1s^{\alpha}}+\frac{R_2}{1+R_2C_2s^{\beta}}+\frac{1}{Ws^{\gamma}}+R_0 \qquad (1)$$

where C_1, C_2, and W represent the parameters of model elements, the fractional orders of the CPE_1 and CPE_2 elements are denoted by α and β , and γ represents the Walberg element fractional order.

In the time domain, the input to the system is $u(t)=I(t)$. The output is $y(t)=U_d(t)-U_{OCV}(t)$. Then the fractional calculus equation of this system model is as follows:

$$\begin{aligned}&(WD^{\gamma}+WR_1C_1D^{\alpha+\gamma}+WR_2C_2D^{\beta+\gamma}+\\&WR_1C_1R_2C_2D^{\alpha+\beta+\gamma})y(t)=[R_1C_1D^{\alpha}+R_2C_2D^{\beta}\\&+(R_0+R_1+R_2)WD^{\gamma}+R_1C_1R_2C_2D^{\alpha+\beta}+\\&(R_0+R_2)WR_1C_1D^{\alpha+\gamma}+(R_0+R_1)WR_2C_2D^{\beta+\gamma}+\\&R_0WR_1C_1R_2C_2D^{\alpha+\beta+\gamma}]u(t)+u(t)\end{aligned} \qquad (2)$$

where parameters D^{α} , D^{β} , D^{γ} , $D^{\alpha+\beta}$, $D^{\alpha+\gamma}$, $D^{\beta+\gamma}$, and $D^{\alpha+\beta+\gamma}$ are fractional-order operators.

According to the derivation process in reference [39], equation (2) can be transformed to the following first-order difference equation:

$$y(k)=-\frac{A(1)}{A(0)}y(k-1)+\frac{1+B(0)}{A(0)}u(k)+\frac{B(1)}{A(0)}u(k-1) \qquad (3)$$

We modeled lithium-ion batteries using fractional calculus theory, as shown in equation (4):

$$D^{1}SOC(t)=\frac{\eta}{C_n}u(t) \qquad (4)$$

In this equation, the battery rated capacity is denoted by C_n, and the battery coulomb efficiency is represented by η .

The system state equation (4) can be discretized as follows:

$$SOC(\mathrm{k}) = SOC(\mathrm{k}-1) + \frac{\eta T}{C_n} u(\mathrm{k}) \quad (5)$$

where T denotes the sampling time.

Equations (3) and (5) can describe the fractional-order ECM of lithium battery. Through the above analysis, the parameters that the model needs to identify are given in equation (6):

$$\theta = [\mathrm{R}_0 \ \mathrm{R}_1 \ \mathrm{C}_1 \ \mathrm{R}_2 \ \mathrm{C}_2 \ \mathrm{W} \ \alpha \ \beta \ \gamma] \quad (6)$$

3. IDENTIFICATION OF FRACTIONAL MODEL PARAMETERS

Because the lithium-ion battery is a time-varying nonlinear system, it is difficult to identify parameters in the battery modeling process. The LS method is based on the principle of minimizing variance, and it is a commonly used mathematical optimization tool. By means of the LS method, the unknown parameters of the system can be quickly obtained based on the established system model, and the sum of squared error between the measured value and the output value of the system model with the identified parameters is minimized At a certain temperature, if the voltage and current data of the battery for charging and discharging is available, the batch-type LS can be employed to identify the parameters of the battery model in one go. However, the computation load of the batch-type LS method is very large, which makes it suitable only for offline parameter calculation. Through the recursive processing of LS method, the RLS method can be used for the recursive calculation according to the sampling order, and it can be used for online parameter identification. The principle of RLS method is that the parameter estimate at the previous step and the new measurement are used to calculate the parameter estimate at the current step. By this means, the parameter estimate is continuously updated through recursion. The RLS is an algorithm that provides the optimal solution of the state equation, by using the data obtained from the input and output of the system through the dynamic linear system state equation. It is a parameter identification method with real-time properties that can be used to update the model parameters of the system [40], moreover, the data needed to be stored is small and the program is simple and easy to implement. Therefore, the RLS is used to update the fractional-order model parameters of lithium-ion batteries in this paper. However, the RLS may produce inaccurate results in the initial stage of parameter identification. The intelligent optimization algorithms, e.g. GA [36], PSO [35], bacterial foraging optimization (BFO) algorithm [41] and other algorithms, which can solve nonlinear and multi-parametric problems, and the parameter identification results are accurate. Compared with GA and BFO, the PSO algorithm is more effective in utilizing processor memory, easier in application and implementation [42]. Hu et al. [23] employed the multi-particle swarm optimization algorithm to identify battery model parameters over the entire battery operating conditions, and the results showed high accuracy and stability. In this study, PSO is improved by adding differential evolution strategy, as suggested in Ref. [43], to promote best-performing particles and improve global optimality. Therefore, the MCPSO intelligent optimization algorithm is used to perform offline parameter identification before online parameter identification is conducted. By this means, the drawback of inaccurate identification in the initial stage of online parameter identification can be overcome.

In order to identify the model parameters, the A123 ternary lithium-ion soft pack batteries were selected as the experimental objects at an ambient temperature of 25 ℃. Table 1 shows the battery

specifications. Using the available lithium-ion power battery test platform (shown in Figure 2), a series of tests were performed. Considering the trade-off between sampling accuracy and data storage load, the sampling time of the battery test system was set to 0.1 s.

Table 1. Battery specifications.

Capacity (Ah)	Charging cut-off voltage (V)	Discharging cut-off voltage (V)	Charging cut-off current (A)	Rated voltage(V)
25	4.20	2.50	1.25	3.60

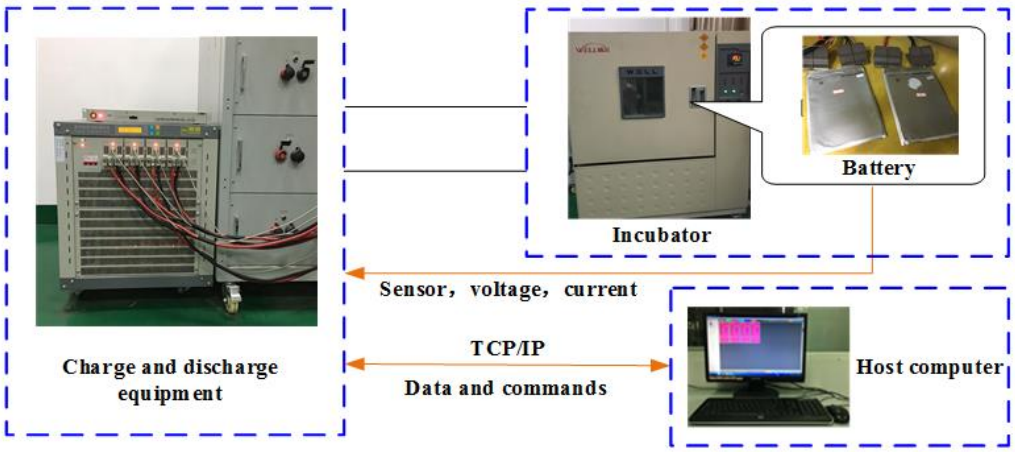

Figure 2. Battery test platform, including incubator, battery test equipment, computer and experimental objects.

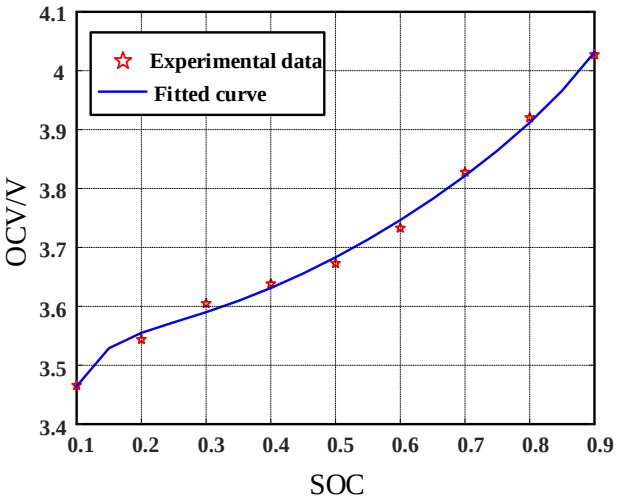

Figure 3. Fitted curve of OCV-SOC.

Firstly, the static capacity test (SCT) was performed to obtain the available capacity of batteries. Next, the hybrid pulse power characteristic (HPPC) test were used to obtain the OCV value at a particular SOC value. According to the empirical equation (7) [44], Figure 3 shows the connection between the OCV and the SOC were obtained by data fitting. The fitting parameters are shown in Table 2. Then based on the MCPSO algorithm, using the experimental data under federal urban driving schedule (FUDS) conditions, offline parameter identification was performed to obtain the initial optimal values of the fractional-order model parameters. The accuracy of the model was verified under the HPPC and dynamic stress test (DST) conditions. Finally, the model parameters were updated online in real time by using RLS, and the model parameters were identified online. The accuracy of the fractional-order model was verified under different cyclic test conditions (i.e. HPPC, DST, and FUDS). The flowchart of online recognition of model parameters based on RLS is shown in Figure 4.

$$U_{OCV}(SOC) = C_0 + C_1 SOC + C_2 \frac{1}{SOC} + C_3 \ln(SOC) + C_4 \ln(1 - SOC) \qquad (7)$$

Table 2. OCV-SOC fitting curve parameter table.

C_0	C_1	C_2	C_3	C_4
2.9520	0.9987	-0.0518	-0.3995	-0.0857

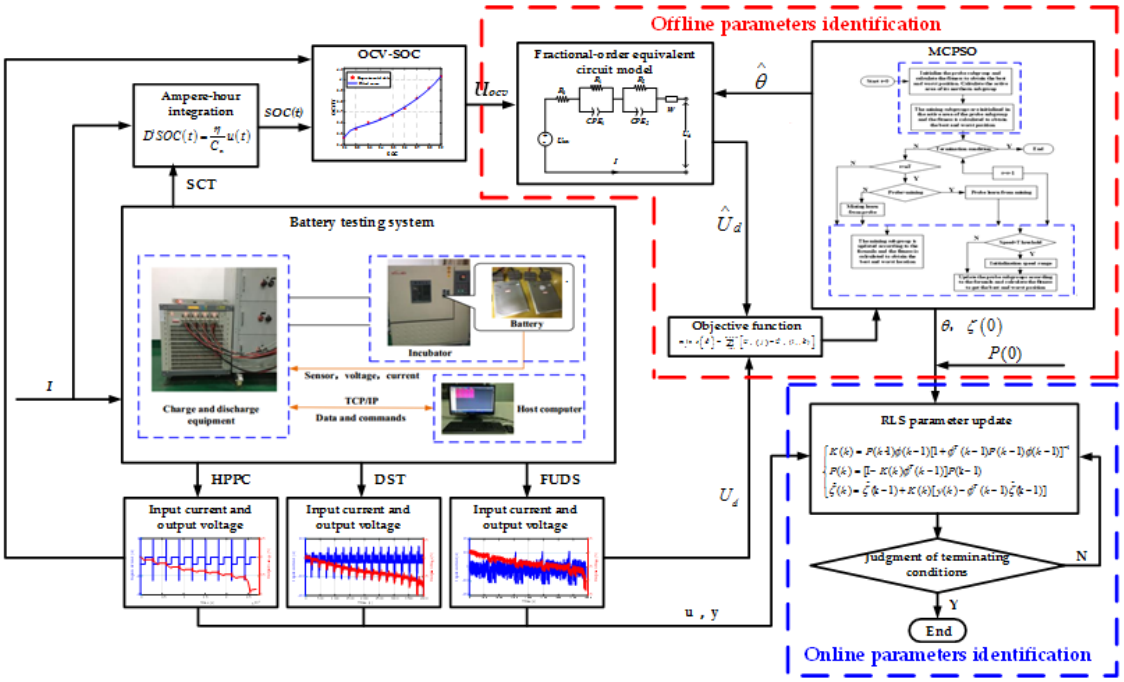

Figure 4. Flow chart of online identification of model parameters based on RLS.

3.1. Offline identification of model parameters

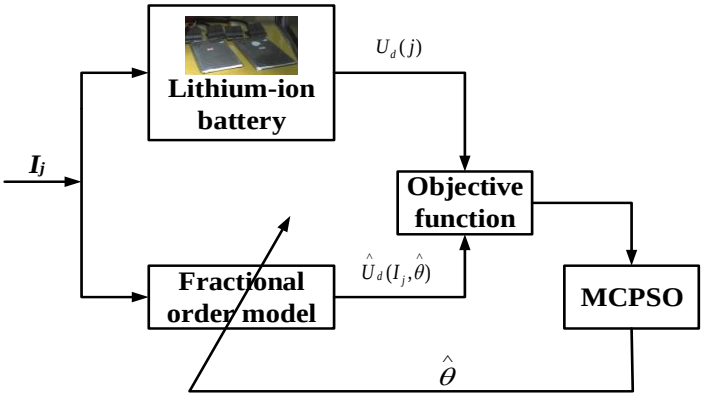

Figure 5. Block diagram of model parameter identification.

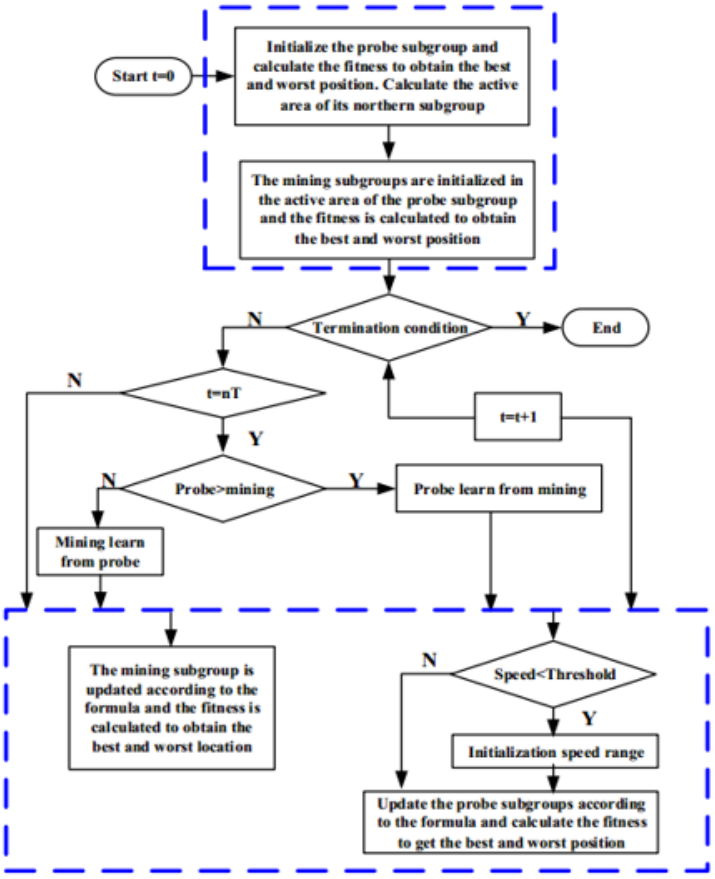

Figure 6. Flow chart for model parameter identification based on MCPSO.

The following equation is the objective function for parameter identification:

$$\min_{\theta} e\left(\hat{\theta}\right) = \sum_{j=1}^{Ndata}\left[U_d\left(j\right) - \hat{U}_d\left(\mathrm{I}_j,\hat{\theta}\right)\right]^2 \qquad (8)$$

In the equation, the fitness function is represented by $e(\hat{\theta})$, $\hat{\theta}$ is the model parameter vector to be identified (defined in equation (6)), the battery voltage measured at the *j*-th sample point is denoted by $U_d(j)$, $\hat{U}_d(I_j,\hat{\theta})$ is the battery voltage estimated based on the identification model output terminal given the input current I_j and model parameter $\hat{\theta}$.

To minimize the error between the model estimated voltage $\hat{U}_d(I_j,\hat{\theta})$ and the battery voltage $U_d(j)$, the parameter vector $\hat{\theta}$ in the fractional-order model is identified through MCPSO. Figure 5 shows the specific identification block diagram.

Table 3. Algorithm parameter.

Dimension	**Size**	**Cooperative time**
9	150	4
Maximum number of generations	**Inertia weight**	**Acceleration factor**
400	0.8-0.3	1.5381

The parameters of the model to be identified are given by equation (6). Figure 6 shows the flow chart of the model parameter identification algorithm based on MCPSO, the specific steps of the algorithm can be found in [39], and the algorithm parameters are shown in Table 3.

The inertia weight decreases linearly from 0.8 to 0.3, and the decline equation is given by:

$$\omega=0.8-\frac{0.3t}{\text{maxgen}} \qquad (9)$$

where t denotes the number of current running generations, ω represents the inertia weight, and the maximum number of generations is represented by maxgen.

3.2. Online parameters identification based on RLS

During actual vehicle operation the battery operating current is large and changes rapidly, which makes it difficult to guarantee the accuracy of model parameter identification. Therefore, battery models and their parameters are normally obtained by offline testing on a test platform before leaving the factory. Practical experience has indicated that the order of the battery model is closely related to the polarization depth, and the model parameters change with SOC, operating conditions, and aging parameters [45]. As a result, using fixed model order and parameters for battery state estimation can lead to large errors. As a result, in this section, the model parameters are adjusted in real time by means of RLS, thereby achieving model parameter online update.

According to equation (3) - the fractional equivalent circuit model difference equation, the input $u(k)$ and output $y(k)$ of the system are extended to n dimensions. A matrix equation can be obtained as equation (10):

$$Y(k)=\Phi(k)\zeta(k)^T+e(k) \qquad (10)$$

where $Y(k)$ represents the observed value, $\Phi(k)$ denotes the parameter matrix, $\zeta(k)$ is the estimated value of the parameter matrix, and $e(k)$ is the measurement noise. The definitions of $\Phi(k)$ and $\zeta(k)$ are given by equation (11), and k denotes the current moment.

$$\Phi=\begin{bmatrix} -y(k-1) & u(k) & u(k-1) \\ -y(k) & u(k+1) & u(k) \\ \mathrm{M} & \mathrm{M} & \mathrm{M} \\ -y(k+n) & u(k+n) & u(k+n-1) \end{bmatrix} \quad \zeta=\begin{bmatrix} \frac{A_k(1)}{A_k(0)} & \frac{1+B_k(0)}{A_k(0)} & \frac{B_k(1)}{A_k(0)} \\ \frac{A_{k+1}(1)}{A_{k+1}(0)} & \frac{1+B_{k+1}(0)}{A_{k+1}(0)} & \frac{B_{k+1}(1)}{A_{k+1}(0)} \\ \mathrm{M} & \mathrm{M} & \mathrm{M} \\ \frac{A_{k+n}(1)}{A_{k+n}(0)} & \frac{1+B_{k+n}(0)}{A_{k+n}(0)} & \frac{B_{k+n}(1)}{A_{k+n}(0)} \end{bmatrix} \tag{11}$$

$$Y=[y(k+1)\ \ y(k+2)\ \mathrm{L}\ \ y(k+n)] \qquad e=[e(k+1)\ \ e(k+2)\ \mathrm{L}\ \ e(k+n)]$$

At time $k-1$ and k, the parameter estimation results obtained by the system are expressed by equation (12):

$$\begin{aligned} \hat{\zeta}(k-1)&=(\Phi(k-1)^T\Phi(k-1))^{-1}\Phi(k-1)^T Y(k-1) \\ \hat{\zeta}(k)&=(\Phi(k)^T\Phi(k))^{-1}\Phi(k)^T Y(k) \end{aligned} \tag{12}$$

At the *k*-th recursion, the parameter estimate $\hat{\zeta}(k-1)$ at time $k-1$, the new observation vector $\Phi(k-1)$ and the actual measurement $y(k)$ have been obtained. New identification parameter $\zeta(k)$ is obtained by formula (13).

$$\begin{cases} K(k)=P(k\text{-}1)\phi(k-1)[1+\phi^T(k-1)P(k-1)\phi(k-1)]^{-1} \\ P(\mathrm{k})=[\mathrm{I}-K(k)\phi^T(k-1)]P(\mathrm{k}-1) \\ \hat{\zeta}(\mathrm{k})=\hat{\zeta}(\mathrm{k}-1)+K(k)[y(k)-\phi^T(k-1)\hat{\zeta}(\mathrm{k}-1)] \end{cases} \tag{13}$$

where $K(k)$ denotes a gain vector and $P(k)$ is defined as $\left(\Phi_k^T\Phi_k\right)^{-1}$.

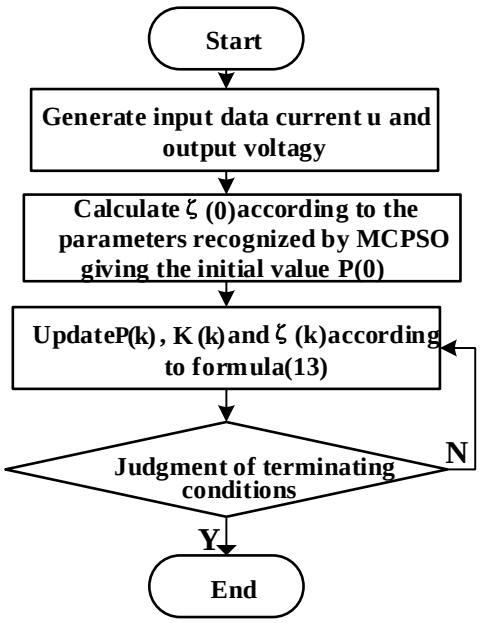

Figure 7. Flow chart of model parameter updating algorithm.

The data needed to be stored is small and the program is simple and easy to implement when the RLS is employed to update the parameters in time. Therefore, the fractional-order model parameters are updated by RLS for lithium-ion batteries in this paper. Figure 7 shows the flow chart of model parameter updating algorithm.

4. SIMULATION VERIFICATION

4.1. Results of offline parameters identification based on MCPSO

The offline parameter identification of the battery model is based on the battery test data. Using the selected battery reference model and experimental test data, the model parameters are optimized through an optimization algorithm. The parameters are used in the later stage by looking up the table or using polynomial fitting. Therefore, in order to obtain accurate battery parameters throughout the battery life cycle, a large number of tests need to be carried out. This paper selects the FUDS test cycle data as the training data for the offline parameter identification. The charging and discharging current and the voltage response of the battery cell A123 under FUDS test cycle condition are shown in Figure 8. The initial battery SOC value is set to 0.65.Taking the FUDS operating current data as the input to the model, based on the MCPSO algorithm, the parameter identification of the fractional-order model is performed and the parameter identification results are shown in Table 4.

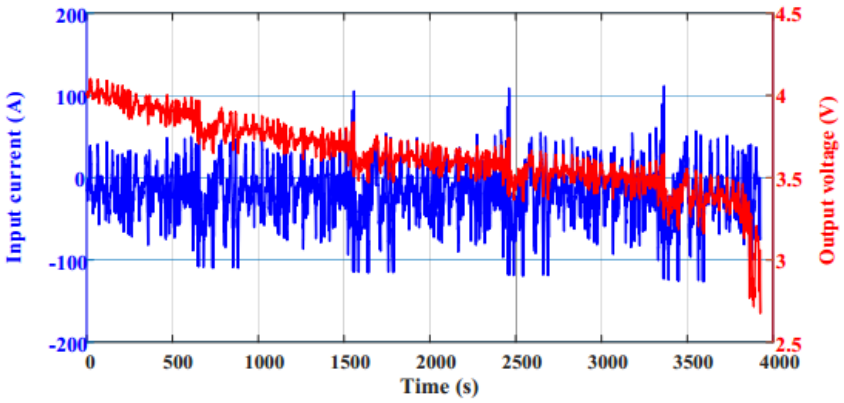

Figure 8. The charging and discharging current and the voltage response of the battery cell A123 under FUDS test cycle condition

Table 4. Fractional model parameter identification results.

R_0	R_1	C_1	R_2	C_2
0.0125	0.0083	19.7142	17.8082	51.1029
W	**α**	**β**	**γ**	
155.7857	0.8386	0.2125	0.1668	

The data in Table 4 is substituted into the established fractional-order model. By inputting the current and voltage data under the FUDS cycle test condition, the output voltage of the model is obtained and compared with the measured voltage, and the verification results of the fractional order model under the experimental data are shown in Figures 9.

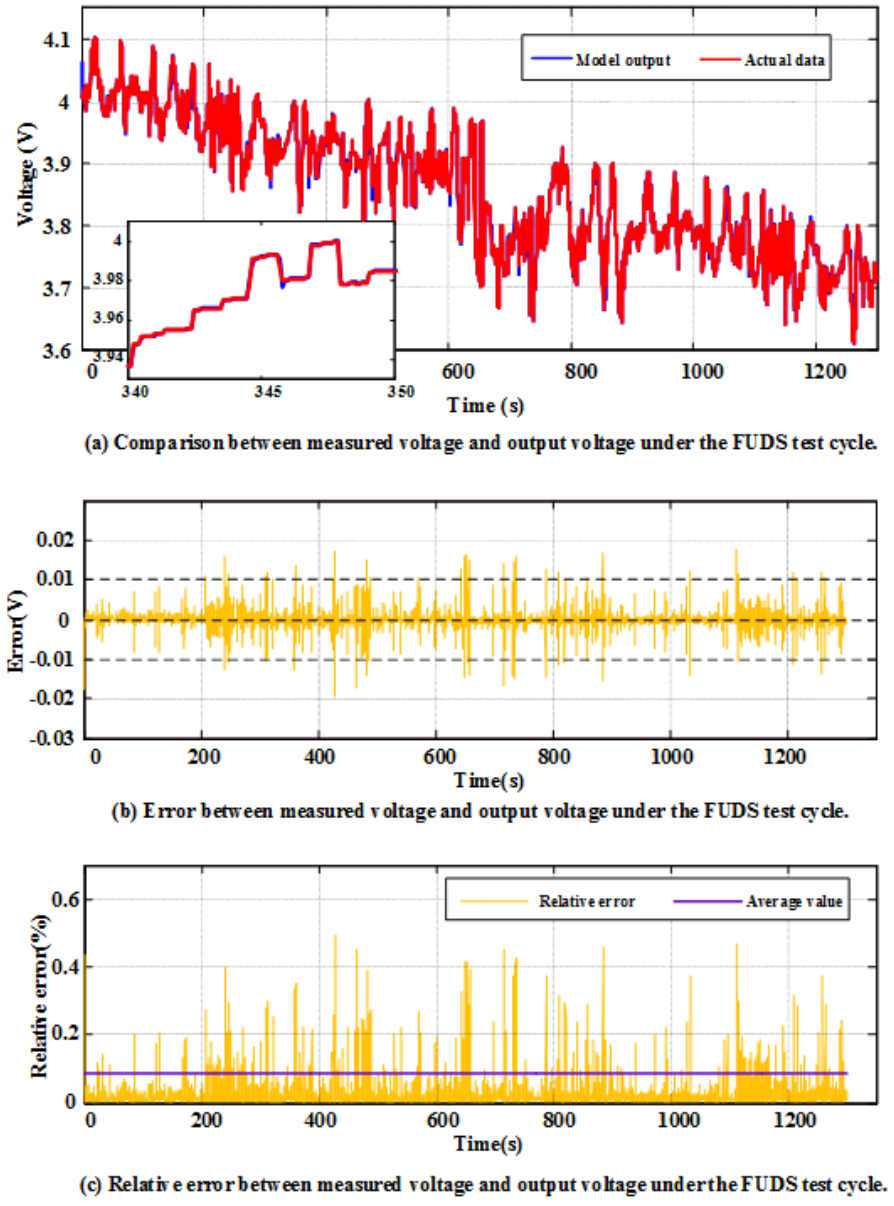

Figure 9. The verification results under the FUDS test cycle.

Figure 9(a) demonstrates that the model output voltage is almost the same as the measured voltage, with the RMSE being 7.66 mV. It is observed in Figure 9(b) that the absolute error almost fluctuates within ± 10 mV, and only when the current changes obviously the error exceeds 20 mV. Besides, Figure 9(c) shows that the average relative error does not exceed 0.1%. In order to better reflecting the accuracy of the fractional-order model established in this study, it is summarized and

compared the model performances of the fractional-order model and reported models as previous reported, such as PNGV model [46], Thevenin model [47], second-order ECM [48]. And the terminal voltage errors comparison results are listed in Table 5. It shows that the fractional-order model has higher accuracy compared with the most reported models. In summary, the accuracy of the fractional-order model for offline parameters identification based on MCPSO is very high.

Table 5. Comparison of terminal voltage errors.

Battery models	RMSE (mV)
Fractional-order model	7.66
PNGV model [46]	35.70
Thevenin model [47]	45.00
Second-order ECM [48]	19.00

4.2. Accuracy verification of fractional order model for off-line identification of parameters

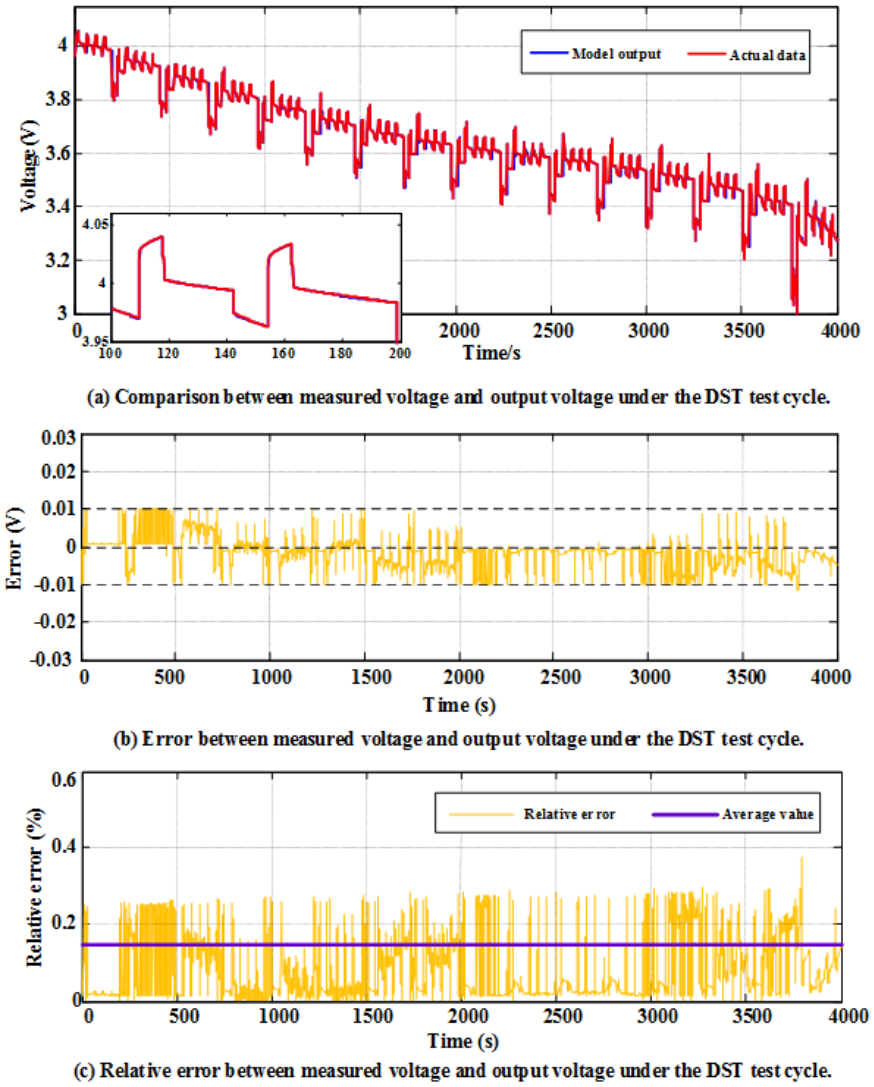

Figure 10. The verification results under the DST test cycle.

In order to study the accuracy of the fractional-order model for offline parameter identification based on MCPSO under the condition of non-training data, the test data under the DST and HPPC operating conditions were selected to illustrate the robustness of the fractional-order model for offline parameter identification based on MCPSO.

The battery is undergone the DST which is close to the actual vehicle running condition. The current and terminal voltage of the battery are measured. The battery test current is used as the model input, and the corresponding model output voltage is obtained. The initial SOC value of the lithium-ion battery is set to 0.9. The verification results under the DST condition is shown in Figure 10.

Figure 10(a) shows that the model provides better fitting between the measured voltage curve and the output voltage curve. Figure 10(b) demonstrates that the absolute error is within ±10 mV, and Figure 10(c) shows that the relative error is within 0.4% with an average of 0.156%. Besides, the estimated RMSE is 8.61 mV, indicating that the model provides close results to the test data under the FUDS and DST operating conditions and presents high accuracy.

Table 6. RMSEs for different test cycles based on MCPSO.

Operating Condition	HPPC	DST	FUDS
RMSE (mV)	9.22	8.61	7.66

The corresponding RMSE tables for different working conditions of fractional order model based on MCPSO are shown in Table 6. Although HPPC, DST and FUDS operating conditions' currents have different frequency changes, Table 6 shows that the RMSE values of the model still don't exceed 10 mV under different conditions, which proves that the fractional-order model for off-line identification of parameters proposed based on MCPSO in this paper has high accuracy and good robustness under different working conditions.

4.3. Accuracy verification of fractional order model for on-line identification of parameters based on RLS

During actual vehicle operation, the model parameters change with SOC, operating conditions, and internal resistance. As a result, using fixed model parameters can lead to large estimation errors. In order to improve the model accuracy and the system adaptability, it is highly necessary to perform online correction and update of the battery model parameters.

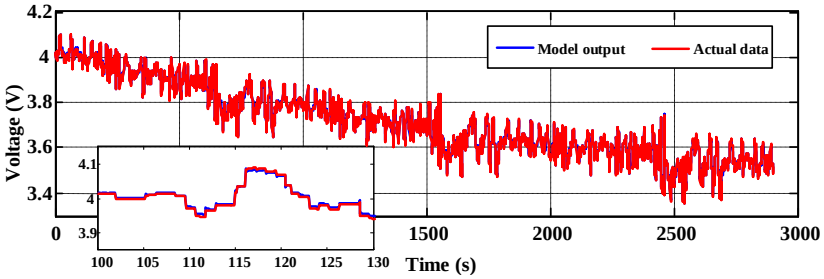

Figure 11. Comparison between measured voltage and output voltage.

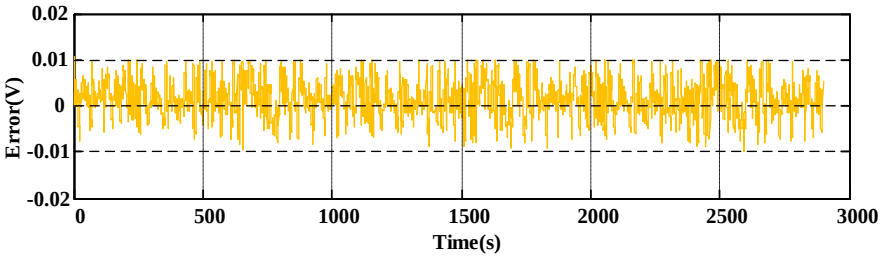

Figure 12. Error between measured voltage and output voltage.

Through the above analysis, the RMSE value of fractional battery model based on off-line parameter identification is less than 10 mV under different working conditions (i.e. HPPC, DST, FUDS). It shows that the fractional battery model based on off-line parameter identification has high accuracy under different working conditions already. Therefore, on this basis, the RLS method is used to update the parameters of the battery model on-line in real-time under different conditions such as FUDS, HPPC and DST (The initial SOC value of lithium-ion battery is set to 0.9), making it more suitable for varying operating conditions of real vehicles. Figure 11 shows a comparison between the model measured voltage and the output voltage under the FUDS cycle test condition. Figure 12 shows the error between the model measured voltage and the output voltage.

Figure 11 shows that the proposed model provides better fitting between the output voltage curve and the measured voltage curve. As observed in Figure 12, the absolute error almost fluctuates within ±10 mV. Compared with the fixed-parameter model error shown in Figure 9, the error in Figure 12 is more moderate. When encountered a large change in current, there is no sudden increase in error. The estimated RMSE is 6.37 mV, which is smaller than the RMSE which is 7.66 mV of the fixed-parameter model under the FUDS. Therefore, the accuracy of the proposed model for on-line identification of parameters has been further improved, and it is able to provide an accurate and stable terminal voltage for SOC estimation, and indirectly guarantee the accuracy of SOC estimation.

Table 7. RMSEs for different test cycles based on RLS.

Operating Condition	HPPC	DST	FUDS
RMSE (mV)	8.37	8.02	6.37

The corresponding RMSE tables for different working conditions of fractional order model based on RLS are shown in Table 7. From this table, we can see that the corresponding RMSE values are smaller in different conditions when compared with Table 6. Under the HPPC cycle test condition, the RMSE value based on the RLS on-line parameter identification of the fractional-order model is 0.85 mV smaller than that based on the MCPSO off-line parameter identification. The RMSE value is reduced by 0.59 mV under the DST cycle test condition, and 1.29 mV under the FUDS cycle test condition. Therefore, it is proved that the fractional-order model for on-line identification of parameters proposed based on RLS in this paper has high accuracy and good robustness under different working conditions when compared with off-line identification of parameters based on MCPSO.

5. CONCLUSIONS

In order to effectively solve the problem of inaccurate identification in the initial stage of the online parameter identification process, in this study, the MCPSO intelligent optimization algorithm is first used to perform offline parameter identification. Then, the RLS method is used to realize online updating of model parameters. The online parameter identification model precisely predicts the changes of battery dynamic terminal voltage, with the absolute error being within 10 mV and the average relative error does not exceed 0.1%. Besides, this model effectively reduces the impacts of battery internal resistance and other parameters to improve the model accuracy. The simulation results show that the on-line parameter identification method proposed in this paper for fractional-order battery model has higher accuracy, better robustness and practicability than the off-line parameter identification method under the same working condition, which provides great potential for enhancing estimation accuracies of SOC and SOH for BMSs.

ACKNOWLEDGEMENTS
This work was supported by the National Key R&D Program of China [No. 2018YFB0106102], and the Major Program of Chongqing Municipality [No. cstc2018jszx-cyztzxX0007].

References

1. Y. Shang, C. Zhang, N. Cui, J.M. Guerrero, *IEEE Trans. Power Electron.*, 30 (2015) 3731.
2. S. Piller, M. Perrin, A. Jossen, *J. Power Sources*, 96 (2001) 113.
3. Z. Song, X. Wu, X. Li, J. Sun, H.F. Hofmann, J. Hou, *IEEE Trans. Power Electron.*, 34 (2019) 7067.
4. W. Su, H. Eichi, W. Zeng, M.-Y. Chow, *IEEE Trans. Ind. Inf.*, 8 (2012) 1.
5. M.H. Amini, O. Karabasoglu, *Energies*, 11 (2018) 196.
6. S. Adams, *Appl. Energy*, 90 (2012) 323.
7. M. Mastali, J. Vazquez-Arenas, R. Fraser, M. Fowler, S. Afshar, M. Stevens, *J. Power Sources*, 239 (2013) 294.
8. J. Meng, D.-I. Stroe, M. Ricco, G. Luo, R. Teodorescu, *IEEE Trans. Ind. Electron.*, 66 (2019) 7717.
9. R. Mingant, J. Bernard, V. Sauvant-Moynot, *Appl. Energy*, 183 (2016) 390.
10. M. Gholizadeh, F.R. Salmasi, *IEEE Trans. Ind. Electron.*, 61 (2014) 1335.
11. C. Zou, X. Hu, Z. Wei, X. Tang, *Energy*, 141 (2017) 250.
12. A. Abdollahi, X. Han, N. Raghunathan, K.R. Pattipati, B. Pattipati, B. Balasingam, Y. Bar-Shalom, B. Card, *J. Storage Mater.*, 9 (2017) 47.
13. H. Aung, J.J. Soon, S.T. Goh, J.M. Lew, K.-S. Low, *IEEE Trans. Aerosp. Electron. Syst.*, 8 (2019) 1.
14. A. Seaman, T.-S. Dao, J. McPhee, *J. Power Sources*, 256 (2014) 410.
15. A. Farmann, D.U. Sauer, *Appl. Energy*, 225 (2018) 1102.
16. T. Zahid, K. Xu, W. Li, *Electron. Lett.*, 53 (2017) 1665.
17. K.T. Chau, K.C. Wu, C.C. Chan, W.X. Shen, *Energy Convers. Manage.*, 44 (2003) 2059.
18. M. Doyle, T. Fuller, J. Newman, *J. Electrochem. Soc.*, 140 (1993) 1526.
19. N. Xue, W. Du, T.A. Greszler, W. Shyy, J.R.R.A. Martins, *Appl. Energy*, 115 (2014) 591.
20. H. He, R. Xiong, J. Fan, *Energies*, 4 (2011) 582.
21. W. Waag, S. Käbitz, D.U. Sauer, *Appl. Energy*, 102 (2013) 885.
22. L. Shi, L. Qiu, X. Huang, F. Zhang, D. Wang, L. Zhou, J. Gao, *Int. J. RF Microwave Comput. Aided*

Eng., 29 (2019) 2168.
23. X. Hu, S. Li, H. Peng, *J. Power Sources*, 198 (2012) 359.
24. C. Yan Ma Xiuwen Zhou Bingsi Li Hong, *Int. J. Automot. Technol.*, 3 (2016) 281.
25. B. Wang, S.E. Li, H. Peng, Z. Liu, *J. Power Sources*, 293 (2015) 151.
26. X. Lin, H.E. Perez, S. Mohan, J.B. Siegel, A.G. Stefanopoulou, Y. Ding, M.P. Castanier, *J. Power Sources*, 257 (2014) 1.
27. H. Wu, S. Yuan, C. Yin, *Int. J. Electr. Eng.*, 192 (2013) 795.
28. L. Zhang, X. Hu, Z. Wang, F. Sun, D.G. Dorrell, *J. Power Sources*, 314 (2016) 28.
29. S.K. Rahimian, S. Rayman, R.E. White, *J. Power Sources*, 196 (2011) 8450.
30. A. Fotouhi, D.J. Auger, K. Propp, S. Longo, *IET Power Electron.*, 10 (2017) 1289.
31. G.L. Plett, *J. Power Sources*, 196 (2011) 2319.
32. X. Tang, X. Mao, J. Lin, B. Koch, *IEEE Eng. Manage. Rev.*, 61 (2014) 1685.
33. M. Partovibakhsh, G. Liu, *IEEE Trans. Control Syst. Technol.*, 23 (2015) 357.
34. Z. Wei, K.J. Tseng, N. Wai, T.M. Lim, M. Skyllas-Kazacos, *J. Power Sources*, 332 (2016) 389.
35. Y. Yao, Y. Wang, X. Liu, Y. Pei, D. Xu, X. Liu, *IEEE Trans. Power Electron.*, 34 (2019) 5268.
36. J.C. Forman, S.J. Moura, J.L. Stein, H.K. Fathy, *J. Power Sources*, 210 (2012) 263.
37. S. Santhanagopalan, Q. Zhang, K. Kumaresan, R.E. White, *J. Electrochem. Soc.*, 155 (2008) A345.
38. T.F. Fuller, T.F. Fuller, M. Doyle, M. Doyle, J. Newman, J. Newman, *J. Electrochem. Soc.*, 141 (1994) 1.
39. M. Hu, Z. Li, Y. Li, S. Li, C. Fu, D. Qin, *Energy*, 165 (2018) 153.
40. H. He, X. Zhang, R. Xiong, Y. Xu, H. Guo, *Energy*, 39 (2012) 310.
41. Y.-P. Chen, Y. Li, G. Wang, Y.-F. Zheng, Q. Xu, J.-H. Fan, X.-T. Cui, *Expert Syst. Appl.*, 83 (2017) 1.
42. Y. del Valle, G.K. Venayagamoorthy, S. Mohagheghi, J.C. Hernandez, R.G. Harley, *IEEE Trans. Evol. Comput.*, 12 (2008) 171.
43. M.G. Epitropakis, V.P. Plagianakos, M.N. Vrahatis, *Information Sciences*, 216 (2012) 50.
44. G.L. Plett, *J. Power Sources*, 134 (2004) 262.
45. W. Gao, Y. Zou, F. Sun, X. Hu, Y. Yu, S. Feng, *J. Power Sources*, 328 (2016) 174.
46. Q. Wang, J. Wang, P. Zhao, J. Kang, F. Yan, C. Du, *Electrochim. Acta*, 228 (2017) 146.
47. R. Xiong, H. He, K. Zhao, *Int. J. Green Energy*, 12 (2015) 272.
48. F.Z. Wen, B. Duan, C.H. Zhang, R. Zhu, Y.L. Shang, J.M. Zhang, *Electronics*, 8 (2019) 834.